Stress Transfer in Shear Deformable Discontinuous Composites

Hong Gun Kim*

(*Received April 13, 1994*)

It is well known that the shear lag theory is not to provide sufficiently accurate strengthening predictions when the fiber aspect ratio is small. This is due to its neglect of stress transfer across the fiber ends and the stress concentrations that exist in the matrix regions near the fiber ends. In this paper, a new approach to investigate stress transfer mechanisms in shear deformable discontinuous composites is proposed to overcome the shortcoming of shear lag theory. The modification scheme is based on the replacement of the matrix between fiber ends with the fictitious fiber to maintain the compatibility of displacement and traction. Thus, the proposed model takes fiber end effects into account and results in fully closed form solutions. It was found that the proposed model gives a good agreement with finite element results and has the capability to correctly predict the values of interfacial shear stresses and local stress variations in the small fiber aspect ratio regime.

Key Words: Shear Lag Theory, Discontinuous Composites, Fiber Aspect Ratio, Fictitious Fiber, Interfacial Shear Stress

1. Introduction

The tensile load applied to a discontinuous fiber or whisker reinforced composite is transferred to reinforcements by a shearing mechanism between the reinforcement and the matrix (Piggot, 1980). One of the earliest attempts to explain the reinforcing effect of fibers was described by Cox (1952), and is now referred to as the shear lag (SL) model which considers long straight discontinuous fibers completely embedded in a continuous matrix. The Cox model was elegant in its simplicity and provides accurate estimates of the elastic modulus increases due to the fibers when the fiber aspect ratio is sufficiently large. Furthermore, the model is also able to provide the variation of internal stresses in both the fiber and matrix and a description of the fiber/matrix interfacial shear stresses in the elastic deformation regime. However, a major shortcoming of the model is its inability to provide sufficiently accurate predictions when the fiber aspect ratio is small. The predicted modulus by the SL model is substantially smaller than the experimentally observed modulus in this regime. This is the regime applicable to major current short fiber or whisker reinforced composites. For example, in SiC whisker reinforced Al alloys, the average aspect ratio is only on the order of four (Arsenault, 1984; Nair et al., 1985; Nutt and Needleman, 1987) for which case the original SL model does not provide adequate descriptions of the stiffening effect of fibers or whiskers as discussed by Taya and Arsenault (1987).

It is the purpose of this paper to provide a strightforward yet rigorous modification of the original SL analysis so as to retain accuracy at small reinforcement aspect ratio values by taking fiber end effects into account. Starting from first principles and using equilibrium and continuity conditions, closed form expressions are provided for the normal stresses at fiber ends and the enhanced local stresses in the matrix end regions. It is demonstrated that the modification not only results in a correct prediction of the fiber stress increases in the small aspect ratio regime when

* Department of Mechanical Engineering, Jeonju University, 1200 Hyoja-Dong 3 Ga, Wansan-Gu, Jeonju 560-759, Korea.

compared to finite element analysis (FEA) results, but is also able to correctly predict the values of interfacial shear stresses and local stress variations in the fiber and matrix. In fact, these local stress values are critical to the analysis of fracture micromechanisms in metal matrix composites (MMCs) as discussed by Murdeshwar (1989).

Subsequent to the Cox model, rigorous elasticity models based on variational approach (Hashin and Shtrikman, 1962, Hashin and Shtrikman, 1963) and self-consistent method (Hill, 1965a) were developed in order to predict the elastic moduli increases in the small aspect ratio regime. The variational method originally developed by Paul (1960) provides proper bounds to the elastic moduli increases but not the local stress values in the fiber and surrounding matrix. In fact, the self-consistent model was first developed by Hershey (1954) and Krone (1958) as a means to model the behavior of polycrystaline materials and an extension of the self-consistent scheme to multiphase media was given by Hill (1965b) and Budiansky (1965). This method provides approximate predictions of composite elastic response that explicitly account for phase geometry. Eshelby's ellipsoidal inclusion method (Eshelby, 1957) is a basic solution of this type and has also been successfully applied to predict both the modulus and yield strength of short fiber composites (Taya and Arsenault, 1987). However, this model is restricted to ellipsoidal reinforcement geometry for which case the internal reinforcement stress is assumed to be uniform. It is well known that for the case of rod-like fiber geometries, uniform reinforcement stresses are obtained only at sufficiently large aspect ratios. The uniform internal reinforcement stress results from the physical nature of the ellopsoidal geometry for which case both normal and shear load transfer to the reinforcement occurs along the entire inclusion/matrix boundary. For an axially aligned cylindrical geometry, however, with the load applied in the axial direction, the normal stress transfer occurs only at the fiber end and the stress transfer along the fiber length is purely of a shear nature. This shear stress transfer gives rise to the known variation of the fiber axial stresses (Piggot, 1980). Accordingly, the SL approach is physically more realistic for fiber geometries provided that fiber end effects can be rigorously accounted for.

There have been limited previous attempts to modify the SL approach. Muki and Sternberg (1969) and Sternberg and Muki (1970) used the SL approach in a more refined manner using integro-differential equations and have calculated the local stresses inside the fiber. However, this model assumed that the fiber center stress is given by the rule of mixture equation applicable strictly only to the long fiber case. Furthermore, Sternberg's results are not able to be applied to obtain expressions for the matrix stress intensification in the fiber end region which provides a significant contribution to the elastic modulus. Recently, Nardone and Prewo (1986) and Nardone (1987) attempted to modify the SL model by assuming that the fiber end stress was equal to the matrix yield stress and further that the matrix average stress was also equal to the matrix yield stress. This made possible an approximate estimate of the macroscopic composite yield strength increase, but this approach is clearly not applicable to the purely elastic regime wherein the elastic modulus increase is to be calculated. Taya and Arsenault (1989) also attempted to modify the original SL approach by assuming that the fiber end stress was equal to the average matix stress, i.e., the stress concentraion at the fiber ends were ignored.

More recently, Kim and Nair (1990) modified the SL analysis by using FEA to provide the fiber end normal stresses. Their results of the predicted internal stress and elastic modulus increases in short fiber reinforced MMCs showed a good agreement with FEA results as well as experimental data. While their work clearly demonstrates that SL solutions have the applicability to the short fiber composite provided fiber end effects are accounted for, the model does not calculate the fiber end stresses from first principles and relies instead on FEA.

The approach in this work involves replacing the matrix region between fiber ends with a fictitious fiber having the same elastic properties as

the matrix and developing conventional SL solutions for both the real and fictitious fiber. Suitable interfacing of these solutions provides the needed results for the local stress and strain values. The model is therfore entirely closed form in nature and does not rely on FEA for any parametric values. An axisymmetric FEA model has been implemented to assess the predictions of the resulting analytical model derived in this paper.

2. Theoretical Development

2.1 Micromechanical model deduced from physical concept

In composites, loads are not directly applied on the fibers but are applied to the matrix material and transferred to the fibers through the fiber ends and also through the cylindrical surface of the fiber near the ends. When the length of a fiber is much greater than the length over which the transfer of stress takes place, the end effects can be neglected. In the case of short fiber composite or discontinuous fiber composite, The end effects cannot be neglected and the composite properties are functions of material and geometrical parameters. The end effects significantly influence the behavior of and reinforcing effects in discontinuous composites. For a good understanding of the behavior of discontinuous composites, it is necessary to first understand the mechanism of stress transfer.

A micromechanical model deduced from physical concept is described as follows. The discontinuous short fibers are considered to be uniaxially aligned with the stress applied in the axial direction of the fibers. The fiber/matrix bond is assumed to be large and no debonding is allowed in keeping with the actual situation in many MMCs (Nair et al., 1985). Further, no plastic yielding is allowed, that is, both matrix and fiber deform in a purely elastic manner. This rationale is an attempt to understand the initial stage of composite behavior. The composite unit cell or representative volume element (RVE) showing the short fiber embedded in a continuous matrix is shown in Fig. 1. The RVE has a length $2L$, diameter D, fiber length $2l$ and fiber diameter d. Note that, hereafter, the axial direction is expressed as x instead of z for convenience.

2.2 Formulation of conventional shear lag model

The free body diagram of an infinitesimal volume having two cross sections is described in Fig. 2. The conventional SL model is based on the concept that fiber tensile stresses are governed by an interfacial shear stress parallel to the fiber surface as shown in Fig. 2. The surface shear force to be in equilibrium with the tensile forces in the fiber is

$$\pi r^2 d\sigma_f = -2\pi r dx \tau_s \tag{1}$$

where $2r\,(=d)$ is the fiber diameter, σ_f is the fiber stress and τ_s is the interfacial shear stress. Note that symbols σ_x and τ_{rx} in Fig. 2 have been switched as σ_f and τ_s, respectively. Hence, rearranging and simplifying

$$\tau_s = -\frac{r}{2}\frac{d\sigma_f}{dx} \tag{2}$$

Shear forces at distance r_1 with those at the fiber surface r in the composite element is

$$2\pi r_1 \tau dx = 2\pi r \tau_s dx \tag{3}$$

Rearranging and simplifying

$$\tau = \frac{r}{r_1}\tau_s \tag{4}$$

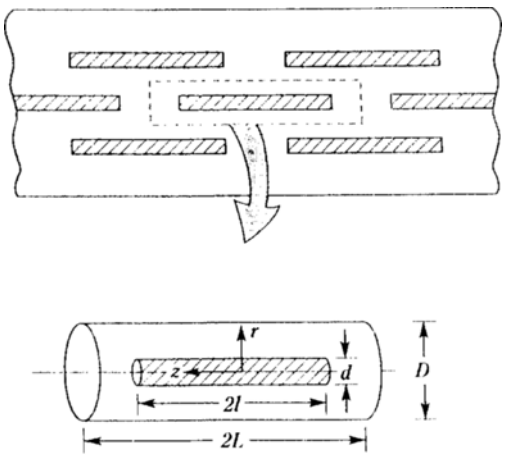

Fig. 1 Composite RVE containing a single fiber in a cylindrical matrix volume

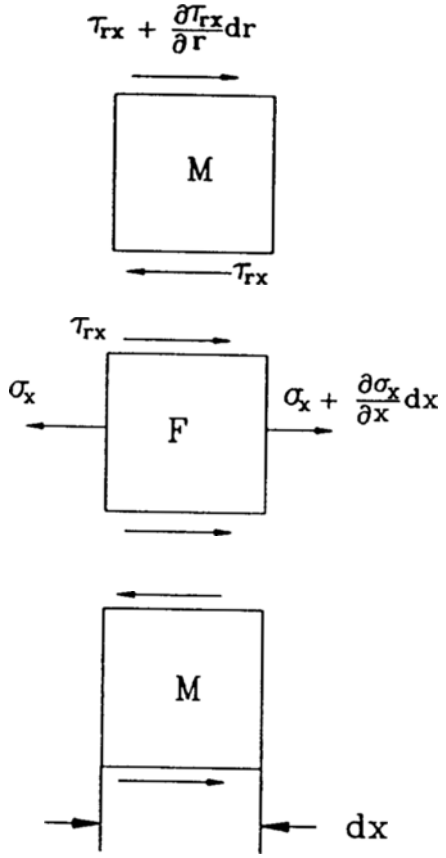

Fig. 2 Free body diagram describing equilibrium condition. F and M represent the fiber and the matrix, respectively

Above two equilibrium conditions (Eqs. (2) and (4)) with Hook's law give the governing differential equation

$$\frac{d^2\sigma_f}{dx^2} = \frac{n^2}{r^2}(\sigma_f - E_f\varepsilon_c) \tag{5}$$

where

$$n^2 = \frac{E_m}{E_f(1+\nu_m)\ln(R/r)} \tag{6}$$

Here, E_m and E_f are Young's moduli of the matrix and fiber, respectively, V_f is the volume fraction of fiver, ε_c is the far-field composite strain and ν_m is the Poisson's ratio of the matrix. As mentioned above, R is the unit cell radius. Eq. (5) has the solution as

$$\sigma_f = E_f\varepsilon_c + A\sinh(nx/r) + B\cosh(nx/r) \tag{7}$$

Here A and B are unknown constants which need to be determined from the following boundary conditions by assuming that no stress is transferred across the fiber ends.

$$\sigma_f = 0 \text{ at } x = \pm L \tag{8}$$

Thus,

$$A = 0 \tag{9}$$

$$B = -\frac{E_f\varepsilon_c}{\cosh(ns)} \tag{10}$$

where $s(=L/r)$ is fiber aspect ratio. Therefore, fiber stress is

$$\sigma_f = E_f\varepsilon_c\left[1 - \frac{1}{\cosh(ns)}\cosh(nx/r)\right] \tag{11}$$

The interfacial shear stress is given by Eqs. (2) and (7):

$$\tau_s = -\frac{n}{2}B\sinh(nx/r) \tag{12}$$

Substituting Eq. (10) into Eq. (12)

$$\tau_s = \frac{nE_f\varepsilon_c\sinh(nx/r)}{2\cosh(ns)} \tag{13}$$

The typical results of the deformation shape, fiber stress and interfacial shear stress are illustrated in Fig. 3.

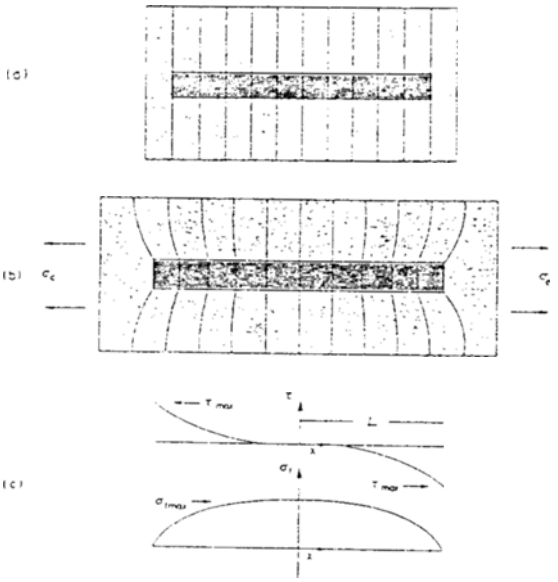

Fig. 3 Single fiber composite element: (a) Unstressed RVE (b) Stressed RVE and (c) The fiber/matrix interfacial shear stress and fiber internal stress for elastic stress transfer

2.3 Derivation of new closed form solutions

In the following derivation of the modified shear lag (MSL) model, the short fibers are also considered to be uniaxially aligned with the stress applied in the axial direction of the fibers. As in the SL model (Cox, 1952) the fiber/matrix bond is assumed to be large and no debonding is allowed for. Finally, in this treatment, residual stress effects are also neglected.

The proposed composite unit cell (RVE) showing the short fiber embedded in a continuous matrix is shown in Fig. 4. The actual, or real, fiber has radius r, and length $2L$. On either end of the fiber is postulated a fictitious fiber also of diameter $2r$ but a length g = half the spacing betweem fiber ends in the composite. The outer surface of the unit cell can be said to have a hexagonal contour, however, the exact shape is not critical in this model. It is treated that the unit cell is an equivalent cylinder with radius R. The spatial variable for the real fiber is x, with the coordinate origin at the fiber center, whereas the spatial variable for the fictitious fiber is x^* with the coordinate origin at the fiber end. The different origins are necessary because, as to be shown, the governing differential equations in the region of the real and fictitious fiber are different and consequently there can be no overlap of the x and x^* domains. The two domains are in contact at $x = L$, or $x^* = 0$, at which point proper boundary conditions need to be applied. Note, in the following, that all variables associated with the fictitious fiber will be denoted with a superscript *. At the far end of the unit cell, that is at the surface $x^* = g$, is applied a uniform constant composite strain ε_c. Under these conditions, as shown in detail in

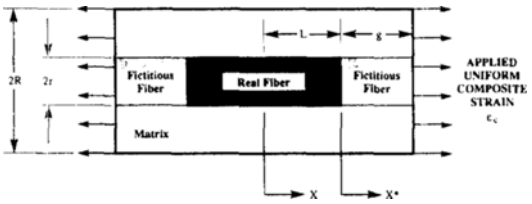

Fig. 4 Schematic of the proposed composite RVE containing a single fiber in a cylindrical matrix volume. Matrix end gap regions were replaced by fictitious fiber

the SL model (Piggot, 1980), the governing equation for the fiber stress, σ_f, and the fiber/matrix interfacial shear stress, τ_s, can be given by the same type as Eqs. (5) and (2), respectively.

In the real fiber regime, Eqs. (1) through (7) are still available except for the constants of Eq. (7) which are needed to be changed. Thus, we have:

$$\sigma_f = E_f\varepsilon_c + C\sinh(nx/r) + D\cosh(nx/r) \tag{14}$$

Here, $C = 0$ due to symmetry and D is the unknown constant which needs to be determined from the following boundary conditions by assuming that the stress is transferred across the fiber ends. By analogy with that for the real fiber, in the fictitious fiber regime, it follows that the governing equation for the fictitious fiber is:

$$\frac{d^2\sigma_f^*}{dx^{*2}} = \frac{n^{*2}}{r^2}(\sigma_f^* - E_f\varepsilon_c^*) \tag{15}$$

Since $E_f^* = E_m$ one obtains

$$n^{*2} = \frac{1}{(1+\nu_m)\ln(R/r)} \tag{16}$$

Therefore, the solution for the fictitious fiber, or the matrix region between fiber ends, is:

$$\sigma_f^* = E_m\varepsilon_c + C^*\sinh(n^*x^*/r) + D^*\cosh(n^*x^*/r) \tag{17}$$

Note that Eq. (17) is a similar form of the solution for the real fiber as shown in Eq. (14). Presumably, the interfacial shear stress for the real fiber is:

$$\tau_s = -\frac{n}{2}D\sinh(nx/r) \tag{18}$$

In the same fashion, we have the solution for the fictitious fiber:

$$\tau_s^* = -\frac{n^*}{2}[C^*\cosh(n^*x^*/r) + D^*\sinh(n^*x^*/r)] \tag{19}$$

Here, $C^* \neq 0$ since the end regions do not possess the symmetry of the fiber because of the coordinate change. Therefore, the three unknown constants in Eq. (17) to (19) are D, C^* and D^*, which can be simply determined using the following boundary conditions. To be satisfied for the displacement and traction compatibility:

$$\sigma_f = \sigma_f^* \text{ at } x = L \text{ or } x^* = 0 \tag{20}$$

$$\frac{d\sigma_f}{dx}=\frac{d\sigma_f^*}{dx^*} \text{ at } x=L \text{ or } x^*=0 \quad (21)$$

$$\tau_s^*=0 \text{ at } x^*=g \quad (22)$$

The first condition sets the fiber/matrix interfacial normal stress at the fiber end to be the same in both regions. The second, requires that the shear stress at the fiber/matrix interface also be the same in the limit $x \to L$ and $x^* \to 0$. These are necessary continuity conditions. The final condition is based on the iso-strain condition of the problem, namely, that the applied strain is uniform across the transverse boundary of the RVE at $x^*=g$. This requires that the shear stress be also zero at $x^*=g$. It can then be shown that the unknown constants are given by:

$$D=\frac{(E_m-E_f)\varepsilon_c}{\cosh(ns)+(n/n^*)\sinh(ns)\coth(n^*s^*)} \quad (23)$$

$$D^*=-D(n/n^*)\sinh(ns)\coth(n^*s^*) \quad (24)$$

$$C^*=-D^*\tanh(n^*s^*) \quad (25)$$

where s $(=L/r)$ is fiber aspect ratio and s^* $(=g/r)$ is the aspect ratio of fictitious fiber. Hence, the fiber maximum stress σ_{fm} can be obtained by setting $x=0$ in Eq. (14):

$$\sigma_{fm}=E_f\varepsilon_c+D \quad (26)$$

In the same manner, the fiber end stress σ_i can also be obtained by setting $x^*=0$ in Eq. (17), namely:

$$\sigma_i=E_m\varepsilon_c+D^* \quad (27)$$

It is important that the stress intensification in the fictitious fiber region is represented by Eq. (27).

3. Description of Numerical Model

The FEA computations were performed using four-noded axisymmetric isoparametric elements (Cook et al., 1989) using ANSYS program (Kohnke, 1989). Provided the fiber or whisker distribution is perfectly uniform, a single fiber model as RVE can be selected (Hashin, 1983) as mentioned above. The RVE selected along with the corresponding mesh patterns are shown in Figs. 5(a) and (b). Two different RVEs were selected, one, based on a single fiber in an quasi-infinite matrix using $V_f=0.5\%$, (Fig. 5(a)), and two, that corresponding to a finite concentration of 20% fibers (Fig. 5(b)). In the latter case, the RVE configuration is similar to that used previously by Agarwal et al. (1974) for a uniform distribution of fiber with an end gap value equal to transverse spacing between fibers. In other words, $g=R-r$. This allows for comparison of volume fraction effects by both FEA and the analytical model developed in the previous section.

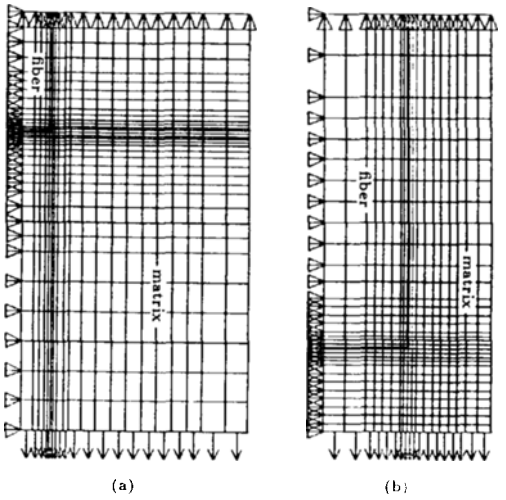

Fig. 5 Axisymmetric FEA meshes of RVE at $s=4$ in case of (a) Quasi-infinite matrix ($V_f=0.5\%$) and (b) Finite Concentration ($V_f=20\%$)

For the boundary conditions, the constraint conditions were imposed by requiring that the longitudinal cell boundary (side wall) and the cell end are undistorted during deformation as implemented in the previous work (Nair and Kim, 1991).

Material properties selected are for Al 2124 as matrix and SiC whisker as reinforcement. For this system, typical values are $E_m=67.2$ GPa, $\nu_m=0.33$ for matrix and $E_f=480$ GPa, $\nu_f=0.17$ for reinforcement (Nair et al., 1985).

4. Results and Discussion

The axial tensile stress in the fiber and matrix end region (fictitious fiber) at 0.1% composite strain is given in Fig. 6 for the case of a single fiber in a quasi-infinite matrix ($V_f=0.5\%$). For

this case, $r=1$, $L=4$, $g=10$, $s=4$, $s^*=10$, $R/r=7.56$, $n=0.2281$, $n^*=0.6097$. The analytical result of this model (MSL) is compared to the FEA results as well as to the prediction of the SL model. As shown in Fig. 6, the fiber stress in the SL model drops to zero as the fiber end region is approached. Further, the tensile stress in the matrix end region in the SL model is assumed constant throughout the gap region and equal to the average matrix stress ($=E_m\varepsilon_c$). On the other hand, in the MSL model the fiber stresses are significantly higher than that in the SL model. These fiber stresses drop off to a finite interfacial value σ_i at the fiber end. The tensile stress in the matrix end region is not constant but decreases from the value at the fiber and approached the SL model predictions at large distances from the fiber end. Further, note that the shape of the fiber tensile stress curve in the MSL model is not the same as that in the SL model because of the different constant values in the SL equation solutions.

For finite fiber concentrations ($V_f=20\%$), the results are shown in Fig. 7. Numerical values were set as $r=1$, $L=4$, $g=1$, $s=4$, $s^*=1$, $R/r=2$, $n=0.3897$ and $n^*=1.0415$. Note from Fig. 7, that the matrix stresses in the end gap region are throughout larger than the average matrix stress, predicted by the SL model. An interfacial value i is also larger than that for the $V_f=0.005$ case. Thus far, fiber end gap stresses and i are increased as the fibers come close together along the axial direction.

The tensile results of the MSL model is in both qualitative and quantitative agreement with the FEA results, both for the single fiber (Fig. 6) and finite fiber concentration cases (Fig. 7). However, note that the maximum stress predicted at the fiber center by the MSL model in Fig. 7 is somewhat higher than the FEA result. This is due to the $ln(R/r)$ term in Eq. (6). The SL and MSL model is clearly invalid as $R\to\infty$ and, in this sense, is similar to the equation for the line tension of dislocations in metallic alloys (Hirth and Lothe, 1980). At more realistic fiber concentrations, the FEA and MSL predictions are in better agreement as shown in Fig. 7. The MSL model is also not applicable in the limit as $R\to r$, for, in this case, as Eq. (7) and Eq. (17) show, the fiber stresses show a singularity.

Interfacial shear stresses at 0.1% composite strain are depicted in Fig. 8 and Fig. 9 for $V_f=0.005$ and $V_f=0.2$, respectively. For the case of the single fiber in an quasi-infinite matrix ($V_f=0.005$), Fig. 8 indicates that the trends in shear

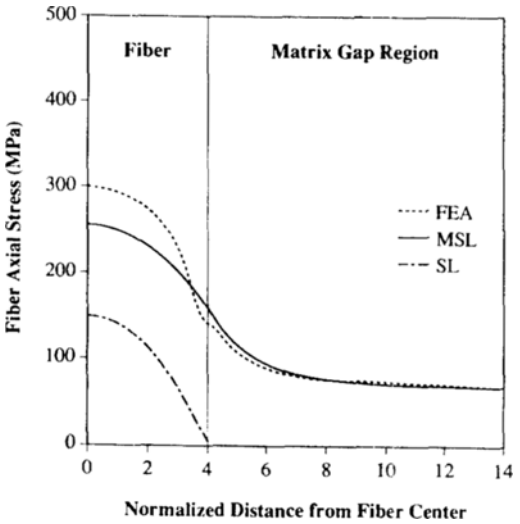

Fig. 6 Real and fictitious fiber axial stress distributions as predicted by SL, MSL and FEA at $\varepsilon_c=0.1\%$ in case of $V_f=0.5\%$

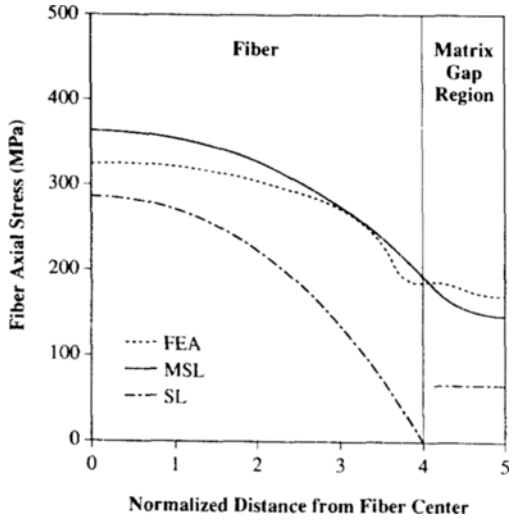

Fig. 7 Real and fictitious fiber axial stress distributions as predicted by SL, MSL and FEA at $\varepsilon_c=0.1\%$ in case of $V_f=20\%$

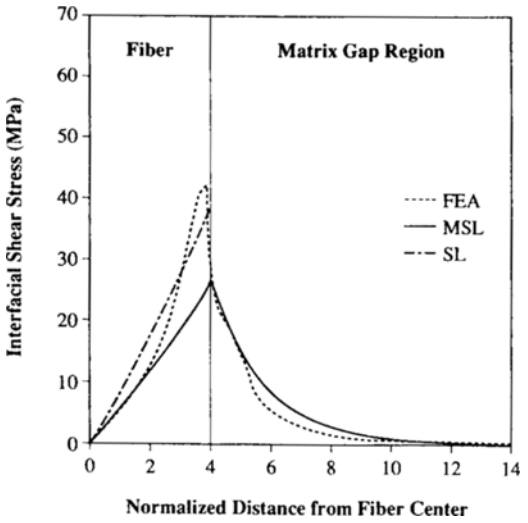

Fig. 8 Interfacial shear stress distributions as predicted by SL, MSL and FEA at $\varepsilon_c=0.1\%$ in case of $V_f=0.5\%$

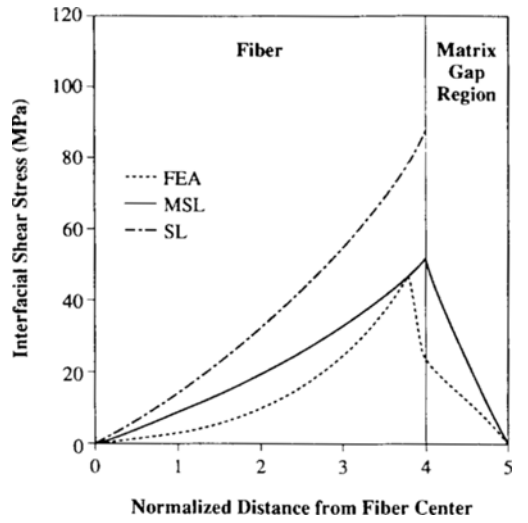

Fig. 9 Interfacial shear stress distributions as predicted by SL, MSL and FEA at $\varepsilon_c=0.1\%$ in case of $V_f=20\%$

stress show good agreement between the MSL model and FEA predictions. Note, however, that the SL model does not provide any shear stress values in the end gap region. The shear stresses at the fiber/matrix interface near the fiber end is somewhat underestimated in the MSL model, again due to the $ln(R/r)$ term as explained earlier. The predicted shear stresses in the gap region by the MSL model agree excellently with calculated FEA results. For the more realistic case of $V_f=0.2$, Fig. 9, there is even better agreement between the FEA shear stress results and that of the MSL model over both the fiber/matrix interface and the matrix gap regions. If local plastic yielding is driven by a Tresca criterion, Fig. 8 and 9 predict that plasticity would progress both into the gap region from the fiber end due to the high shear stresses there as well as towards the fiber center from the fiber corners because of the high shear stresses at the fiber/matrix interfaces near the fiber end. Consequently, plastic yielding of the composite would commence at stresses lower than the macroscopic matrix yield stress. These shear stress values can then be used to estimate the approximate size of locally yielded zones around the short fiber ends. The extension to the elasto-plastic behavior will be the subject of a subsequent paper.

On the other hand, the maximum fiber stress, as shown in Eq. (26) and Fig. 10, is proportional to macroscopic composite strain. Consequently, at composite strain close to the matrix yield strain

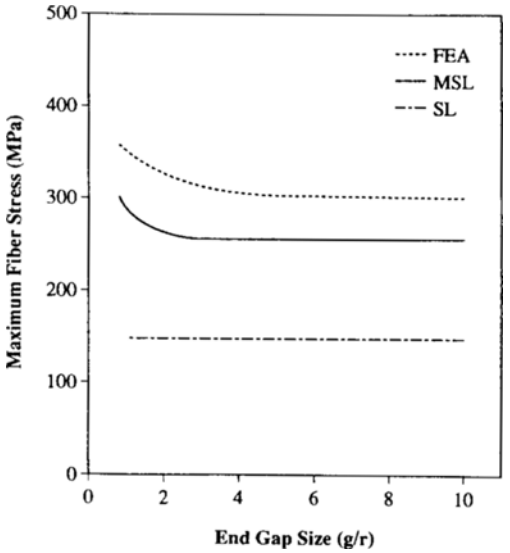

Fig. 10 Fiber maximum stresses predicted by SL, MSL and FEA as a function of end gap size at $\varepsilon_c=0.1\%$ in case of $V_f=0.5\%$

(~0.5%) for SiC reinforced Al 2124, the maximum fiber stress can be well over 1 GPa. Further, it is also dependent on the end gap size as shown in Fig. 10. The results are again comparable with FEA and show that the fiber stresses are enhanced when the end gap size is reduced. The high stress intensification at the fiber center compared to SL predictions is important from the standpoint of potential fiber fracture during deformation of MMCs. Preliminary result by Murdeshwar (1989) suggests that fibers may actually fracture during tensile straining of a SiC whisker reinforced aluminum alloy. The intensification of stresses in the matrix end region is also important from the standpoint of early plasticity of stresses in the matrix end region during deformation of the composite. A fracture mechanism proposed by Nutt and Needleman (1987) involves the nucleation of voids in fiber end regions due to the stress intensification there resulting in lower ductility values for the short fiber reinforced MMC.

5. Conclusions

The disadvantage of the conventional shear lag model was rigorously modified by coupling the fiber to the associated matrix end regions by introducing fictitious fiber concept. The results provide closed form solutions for the predicted local tensile and shear stress values in the fiber and matrix. The qualitative and quantitative results of local stress predictions match FEA results fairly well. When the fiber aspect ratio is sufficiently large the modulus predictions of modified shear lag model correctly approach those of the original shear lag analysis as it should. It was found that the shear lag concept is useful and simple enough to predict microscopic stress and strain variations if the accuracy is increased by a reasonable modification.

References

Agarwal, B. D., Lifsitz, J. M. and Broudtman, L. J., 1974, "Elastic-Plastic Finite Element Analysis of Short Fiber Composites," *Fiber Science and Technology*, Vol. 7, pp. 45~62.

Aresenault, R. J., 1983, "Interfaces in Metal Matrix Composites," *Scripta Metallurgica*, Vol. 18, pp. 1131~1134.

Arsenault, R. J., 1984, "The Strengthening of Aluminum Alloy 6061 by Fiber and Platelet Silicon Carbide," *Materials Science and Engineering*, Vol. 64, pp. 171~181.

Budiansky, B., 1965, "On the Elastic Modulus of Some Heterogeneous Materials," *Journal of the Mechanics and Physics of Solids*, Vol. 13, pp. 223~227.

Cook, R. D., Malkua, D. S. and Plesha, M. E., 1989, *Concepts and Applications of Finite Element Analysis*, John Wiley and Sons, Third Edition, pp. 163~295.

Cox, H. L., 1952, "The Elasticity and Strength of Paper and Other Fibrous Materials," *British Journal of Applied Physics*, Vol. 3, pp. 72~79.

Eshelby, J. D., 1957, "The Determination of the Elastic Field of an Ellipsoidal Inclusion and Related Problems," *Proceedings of the Royal Society, London*, Vol. A241, pp. 376~396.

Halpin, J. C., 1984, *Primer on Composite Materials : Analysis*, Technomic Publishing Co., Inc., pp. 130~141.

Halpin, J. C. and Kardos, J. L., 1976, "The Halpin-Tsai Equations : A Review," *Polymer Engineering and Science*, Vol. 16, No. 5, pp. 344~352.

Hashin, Z., 1983, "Analysis of Composite Materials," *Journal of Applied Mechanics*, Vol. 50, pp. 481~505.

Hashin, Z. and Shtrikman, S., 1962, "On Some Variational Principles in Anisotropic and Nonhomogeneous Elasticity," *Journal of the Mechanics and Physics of Solids*, Vol. 10, pp. 335~332.

Hashin, Z. and Shtrikman, S., 1963, "A Variational Approach to the Theory of the Elastic Behavior of Multiphase Materials," *Journal of the Mechanics and Physics of Solids*, Vol. 11, pp. 127~140.

Hershey, A. V., 1954, "The Elasticity of an Isotropic Aggregate of an Anisotropic Cubic Crystals," *Journal of Applied Mechanics*, Vol. 21, pp. 236~240.

Hill, R., 1965a, "Theory of Mechanical Prop-

erties of Fiber-Strengthened Materials-III, Self-Consistent Model," *Journal of the Mechanics and Physics of Solids*, Vol. 13, pp. 189~198.

Hill, R., 1965b, "A Self-Consistent Mechanics of Composite Materials," *Journal of the Mechanics and Physics*, Vol. 13, pp. 213~222.

Hirth, J. P. and Lothe, J., 1982, *Theory of Dislocations*, John Wiley and Sons, Inc., pp. 79~81.

Kim, H. G. and Nair, S. V., 1990, "Strengthening Analysis of SiC Whisker Reinforced Aluminum Alloys," *Proceedings of the 11th World Korean Scientists and Engineers Conference, The Korean Federation of Science and Technology Societies*, Seoul, Korea, June. 25~29, pp. 1737~1742.

Kohnke, P. C., 1989, *ANSYS Theoretical Manual, 5th Edition*, Swanson Analysis Systems Inc., Houston, PA.

Kroner, E., 1958, "Berechnung del Elastischen Konstanten des Vielkristalls aus den Konstanten del Einkristalls," *Zeitschrift fur Physik*, Vol. 151, pp. 504~518.

Muki, R. and Sternberg, E., 1969, "On the Diffusion of an Axial Load fron an Infinite Cylindrical Bar Embedded in an Elastic Medium," *International Journal of Solids and Structures*, Vol. 5, pp. 587~605.

Murdeshwar, N., 1989, "Fracture Development in a 20 Volume Percent Silicon Carbide Whisker Reinforced Al 2124 Metal Matrix Composite," M. S. Thesis, University of Massachusetts at Amherst.

Nair, S. V., Tien, J. K. and Bates, R. C., 1985 "SiC-Reinforced Aluminum Metal Matrix Composites," *International Metals Review*, Vol. 30, No.6, pp. 275~290.

Nair, S. V. and Kim, H. G., 1991, "Thermal Residual Stress Effects on Constitutive Response of a Short Fiber or Whisker Reinforced Metal Matrix Composite," *Scripta Metallurgica*, Vol. 25, No. 10, pp. 2359~2364.

Nardone, V. C., 1987, "Assessment of Models Used to PRedict the Strength of Discontinuous Silicon Carbide Reinforced Aluminum Alloys," *Scripta Metallurgica*, Vol. 21, pp. 1313~1318.

Nardone, V. C. and Prewo, K. M., 1986, "On the Strength of Discontinuous Silicon Carbide Reinforced Aluminum Composites," *Scripta MEtallurgica*, Vol. 20, pp. 43~48.

Nutt, S. R. and Needleman, A., 1987, "Void Nucleation at Fiber Ends in Al-SiC Composites," *Scripta Metallurgica*, Vol. 21, pp. 705~710.

Paul, B., 1960, "Prediction of Elastic Constants of Multiphase Materials," *Transaction of the Metallurgical Society of AIME*, Vol. 218, pp. 36~46.

Piggot, M. R., 1980, "Load Bearing Fiber Composites," *Pergamon Press*, pp. 83~99.

Sternberg, E. and Muki, R., 1970, "Load-Absorption by a Filament in Fiber Reinforced Material," *Journal of Applied Mathematics and Physics (ZAMP)*, Vol. 21, pp. 552~569.

Tandon, G. P. and Weng, G. J., 1986, "Stress Distribution In and Around Spheroidal Inclusions and Voids at Finite Concentration," *Journal of Applied Mechanics*, Vol. 53, pp. 511~518.

Taya, M. and Arsenault, R. J., 1987, "A Comparison between a Shear Lag Type Model and an Eshelby Type Model in Predicting the Mechanical Properties of Short Fiber Composite," *Scripta Metallurgica*, Vol. 21, pp. 349~354.

Taya, M. and Aresenault, R. J., 1989, "Metal Matrix Composites : Thermomechanical Behavior," *Pergamon Press*, pp. 25~28.